



**HAL**  
open science

## **XANES study of the oxidation state of Cr in lower mantle phases: Periclase and magnesium silicate perovskite**

Sigrid Griet Eeckhout, Nathalie Bolfan-Casanova, Catherine Mccammon, Stephan Klemme, Elodie Amiguet

### ► To cite this version:

Sigrid Griet Eeckhout, Nathalie Bolfan-Casanova, Catherine Mccammon, Stephan Klemme, Elodie Amiguet. XANES study of the oxidation state of Cr in lower mantle phases: Periclase and magnesium silicate perovskite. *The American Mineralogist*, 2007, 92 (5-6), pp.966-972. 10.2138/am.2007.2318 . hal-00328944

**HAL Id: hal-00328944**

**<https://hal.science/hal-00328944>**

Submitted on 5 Dec 2017

**HAL** is a multi-disciplinary open access archive for the deposit and dissemination of scientific research documents, whether they are published or not. The documents may come from teaching and research institutions in France or abroad, or from public or private research centers.

L'archive ouverte pluridisciplinaire **HAL**, est destinée au dépôt et à la diffusion de documents scientifiques de niveau recherche, publiés ou non, émanant des établissements d'enseignement et de recherche français ou étrangers, des laboratoires publics ou privés.

# XANES study of the oxidation state of Cr in lower mantle phases: Periclase and magnesium silicate perovskite

SIGRID GRIET ECKHOUT,<sup>1,\*</sup> NATHALIE BOLFAN-CASANOVA,<sup>2</sup> CATHERINE MCCAMMON,<sup>3</sup>  
STEPHAN KLEMME,<sup>4</sup> AND ELODIE AMIGUET<sup>2</sup>

<sup>1</sup>European Synchrotron Radiation Facility, 6 rue J. Horowitz, BP220, F-38043 Grenoble, France

<sup>2</sup>University of Clermont-Ferrand, 5 rue Kessler, F-63038 Clermont-Ferrand, France

<sup>3</sup>Bayerisches Geoinstitut, Universität Bayreuth, D-95440 Bayreuth, Germany

<sup>4</sup>CSEC and School of GeoSciences, University of Edinburgh, West Mains Road, Edinburgh EH9 3JW, U.K.

## ABSTRACT

Cr *K*-edge X-ray absorption near-edge structure (XANES) spectra were recorded on Cr:MgO periclase and Cr:(Mg,Fe)O ferropericlase synthesized at different pressures (4 and 12 GPa) and temperatures (1200 to 1400 °C) at reducing oxygen fugacity conditions (~iron-wüstite buffer IW to IW – 2), and on Cr:MgSiO<sub>3</sub> perovskite with 0.5 wt% Cr<sub>2</sub>O<sub>3</sub>. <sup>57</sup>Fe Mössbauer spectra were collected on the Fe-containing samples. The aim of the study was to determine the Cr oxidation state in phases found in the Earth's lower mantle, and to examine the possible relationship with the Fe oxidation state in the same materials. To calculate the amount of Cr<sup>2+</sup>, the intensity of the shoulder at the low-energy side of the edge crest was quantified using the area of the corresponding peak in the derivative XANES spectra (Berry and O'Neill 2004). In Cr:(Mg,Fe)O the relative Cr<sup>2+</sup> content reached at most 12.5% but results from Mössbauer spectroscopy combined with chemical composition data suggest that some Cr<sup>2+</sup> oxidized during cooling through the reaction Cr<sup>2+</sup> + Fe<sup>3+</sup> → Cr<sup>3+</sup> + Fe<sup>2+</sup>. In iron-free Cr:MgO, the Cr<sup>2+</sup> content is much higher and reaches ~40%. In Cr:MgSiO<sub>3</sub> perovskite with 0.006 Cr pfu (similar to estimated lower mantle abundance), chromium is mainly divalent.

**Keywords:** XANES, Cr oxidation state, ferropericlase, periclase, Cr:MgSiO<sub>3</sub> perovskite

## INTRODUCTION

Previous trace-element studies report that minor amounts of Cr are present in the Earth's mantle in an oxidized form (~0.3 wt% Cr<sub>2</sub>O<sub>3</sub> is believed to be present in the primitive mantle, from O'Neill and Palme 1998). Chromium is mostly found as Cr<sup>3+</sup> and Cr<sup>6+</sup> in Earth materials, and the only natural occurrence of Cr<sup>2+</sup> was observed in lunar basalts (Sutton et al. 1993). However, Berry et al. (2003) have recently shown that in the presence of iron and at high temperatures, Cr<sup>2+</sup> is not quenchable because of electron charge transfer with Fe<sup>3+</sup> upon cooling. Changes in the oxidation state of transition elements have been predicted to be induced by high pressure (Li et al. 1995) but have not been verified experimentally, even though such changes would be critical for their partitioning behavior during differentiation processes. Also, the valence state of transition elements in ferropericlase is important because these elements play a role in properties such as electrical conductivity (Dobson and Brodholt 2000), ionic diffusion (Mackwell et al. 2005), H solubility (Bolfan-Casanova et al. 2003), thermal conductivity through radiative heat transfer (Goncharov et al. 2006), and lower mantle oxygen fugacity (McCammon et al. 2004).

To better understand the factors controlling the incorporation of chromium in mantle materials, we investigated the crystal

chemistry of Cr in synthetic high-pressure Cr:MgO periclase, Cr:(Mg,Fe)O ferropericlase, and Cr:MgSiO<sub>3</sub> perovskite using X-ray absorption near-edge structure (XANES). We focused on pre-edge features, which strongly depend on the valence state and coordination number of transition elements (Calas and Petiau 1983; Farges et al. 2001; Giuli et al. 2003, 2004; Sutton et al. 2005; Westre et al. 1997; Wilke et al. 2001). Additional <sup>57</sup>Fe Mössbauer spectra were performed on the Fe-containing samples to examine the relationship between the oxidation state of Cr and Fe.

## EXPERIMENTAL METHODS

Two starting materials were used for the high-pressure synthesis of Cr-bearing periclase: one containing iron, of nominal composition Mg<sub>82.5</sub>Fe<sub>16.0</sub>Ni<sub>1.0</sub>Cr<sub>0.5</sub>O<sub>100</sub>, and another one without iron, Mg<sub>97.5</sub>Cr<sub>2.5</sub>O<sub>100</sub>, both prepared from mixing oxides MgO, fired at 1000 °C for 12 h, Fe<sub>2</sub>O<sub>3</sub>, NiO, Cr<sub>2</sub>O<sub>3</sub> and metallic Fe and Cr. Iron was incorporated in the form of Fe<sub>2</sub>O<sub>3</sub> and Fe in the molar ratio of 1:2.5 to provide excess metallic Fe for maintaining low oxygen fugacity. Cr was added in the form of Cr<sub>2</sub>O<sub>3</sub> and Cr in the molar ratio 2:1. Divalent chromium should be stable at oxygen fugacities below the iron-wüstite buffer (Papike et al. 2005). The high-pressure samples were synthesized in a 1000 ton multi-anvil press at the Laboratoire Magmas et Volcans, Clermont-Ferrand, France. MgO octahedral pressure cells of 25 and 14 mm edge length were used for experiments at 4 and 12 GPa, respectively. Different configurations were adopted depending on the composition of the samples. Metallic iron capsules were used inside a LaCrO<sub>3</sub> furnace (*f*<sub>O<sub>2</sub></sub> slightly below the iron-wüstite buffer, since both phases were still present after the experiment), and graphite capsules in a Re furnace. Both configurations are expected to exert reducing conditions on the samples (Table 1), but the graphite capsule does not contaminate the sample. After the experiment, the iron capsule almost disappeared

\* E-mail: eckhout@esrf.fr

**TABLE 1.** Area of the absorption edge shoulder (a.u.) and Cr<sup>2+</sup> concentration (%) for the Cr reference, Cr:MgSiO<sub>3</sub> perovskite, and Cr:MgO periclase samples, calculated as Cr<sup>2+</sup> (at%) = Cr<sup>2+</sup>/(Cr<sup>2+</sup> + Cr<sup>3+</sup>) × 100

	Area (a.u.)	Fit agreement index (%)	Cr <sup>2+</sup> (%)	Fe <sup>3+</sup> (%)	Composition of run products	Capsule	P (GPa)	T (°C)	Furnace
chromite	0.000	99.4	0.00						
ferropericlase 400	0.007	98.6	1.59	2(2)	Mg <sub>83(1)</sub> Fe <sub>17(1)</sub> Ni <sub>0.23(7)</sub> Cr <sub>0.54(3)</sub> O <sub>100</sub> + Fe <sub>96(4)</sub> Ni <sub>14(4)</sub> Cr <sub>0.21(3)</sub>	Fe	12	1200	LaCrO <sub>3</sub>
ferropericlase 403	0.009	99.4	2.07	5(2)	Mg <sub>85(1)</sub> Fe <sub>14(1)</sub> Ni <sub>0.12(6)</sub> Cr <sub>0.6(1)</sub> O <sub>100</sub> + Fe <sub>80(1)</sub> Ni <sub>19(1)</sub> Cr <sub>0.17(2)</sub>	Fe	4	1200	LaCrO <sub>3</sub>
ferropericlase 401	0.052	97.6	12.50	1(2)	Mg <sub>83(1)</sub> Fe <sub>16(1)</sub> Ni <sub>0.5(2)</sub> Cr <sub>0.59(3)</sub> O <sub>100</sub> + not analyzed	Fe	12	1400	LaCrO <sub>3</sub>
periclase 410	0.143	99.7	34.38		Mg <sub>96.9(1)</sub> Cr <sub>3.0(1)</sub> O <sub>100</sub> + Cr metal	C	10	1200	Re
periclase 404	0.171	99.8	41.11		Mg <sub>97.7(1)</sub> Cr <sub>2.3(1)</sub> O <sub>100</sub> No metal observed	C	12	1300	Re
perovskite	0.291	99.5	69.95		Mg <sub>1.001(8)</sub> Si <sub>0.993(7)</sub> Cr <sub>0.006(1)</sub> O <sub>3</sub>	Pt	25	1650	LaCrO <sub>3</sub>
enstatite	0.416	99.4	100.00		Mg <sub>0.90(2)</sub> Cr <sub>0.10(2)</sub> SiO <sub>3</sub>	Glass ampoule	1 atm	1350	Glass ampoule

Note: Estimated values of Fe<sup>3+</sup>/ΣFe determined by Mössbauer spectroscopy are also included, as well as information on the synthesis conditions.

because of the reaction to form ferropericlase. Heating durations ranged from 60 to 330 minutes. For the XANES measurements, a portion of the sample was ground and the metal fraction was removed as much as possible using a magnet. After XANES and Mössbauer measurements, the remainder of the samples were embedded in epoxy and polished for electron microprobe analysis (Table 1) and textural observation using SEM. The standards used were MgO, Cr<sub>2</sub>O<sub>3</sub>, Fe, and NiO, with counting times of 30 s for Mg and Cr and 20 s for Fe and Ni. Most samples consisted of three phases: periclase/ferropericlase, metal arising from the capsule material, and excess metal reacted from the starting powders, except in the case of sample 404 for which no metal was observed. The periclase crystals were polygonal, consistent with textural equilibrium and showed a homogeneous composition. In the presence of Fe, Ni, and Cr, the metallic phase was an alloy of the three elements, distributed as small blebs, and was usually difficult to analyze with the electron beam. Even when the metallic phases were clearly observed in SEM images, the metal fractions could not be detected using our X-ray powder diffraction equipment (Sigma 2080, Cu tube). Image analysis of the SEM pictures indicates metal fractions on the order of 1–5% (area) of the surface. Regarding the composition of the metal phase, we note a decrease in the partitioning of Ni between the oxide and the metal phase at 4 GPa and 1200 °C compared to the sample synthesized at 12 GPa and 1200 °C (Table 1). This observation is in agreement with previous literature data showing that Ni becomes less siderophile with increasing pressure (Li and Agee 1996), and supports the conclusion that equilibrium was achieved between metallic and oxide phases.

The Cr:MgSiO<sub>3</sub> perovskite sample was made from the oxide mixtures MgO, SiO<sub>2</sub>, Cr<sub>2</sub>O<sub>3</sub>, and Mg(OH)<sub>2</sub> to provide 0.5 wt% H<sub>2</sub>O. The Cr content is close to that of the primitive mantle (0.38 wt%, Allègre et al. 1995). The synthesis was performed at 25 GPa and 1650 °C using the 10/4 assembly with a Pt capsule and a LaCrO<sub>3</sub> furnace at Bayerisches Geoinstitut, Bayreuth, Germany. The run product composition was measured using the electron microprobe to be Mg<sub>1.001(8)</sub>Si<sub>0.993(7)</sub>Cr<sub>0.006(1)</sub>O<sub>3</sub> as measured on 20 points, with Mg/Si of 1.01 ± 0.02. While Cr-bearing periclase displayed a greenish to brown color, Cr-doped MgSiO<sub>3</sub> perovskite was of an intense orange color.

Synthetic Cr<sup>2+</sup>-bearing enstatite with composition Mg<sub>0.9</sub>Cr<sub>0.1</sub>SiO<sub>3</sub> was prepared by sintering high-purity oxides at 1350 °C in evacuated double SiO<sub>2</sub>-glass ampoules. Starting materials consisted of high-purity MgO (99.9%), SiO<sub>2</sub> (99.999%), Cr (99.9%), and Cr<sub>2</sub>O<sub>3</sub> (99.999%). MgO, SiO<sub>2</sub>, and Cr<sub>2</sub>O<sub>3</sub> starting materials were fired at 1000 °C to remove any unwanted hydroxide or carbonate and subsequently stored at 110 °C in a vacuum furnace. The starting materials were mixed in an agate mortar under acetone and pressed into small pellets. The pellets were stored in a vacuum furnace at 150 °C for at least 24 h to remove all acetone. Subsequently, the pellets were sealed in small evacuated SiO<sub>2</sub>-glass ampoules. These small ampoules were welded in larger evacuated SiO<sub>2</sub>-glass ampoules. The ampoules were fired for 24 h at 1350 °C in a conventional vertical high-temperature furnace. The ampoules were quench-dropped into distilled water. The sintered Cr-bearing enstatite pellets were compact and had a bluish color. X-ray diffraction (XRD; detection limit of 1–3%) showed enstatite only. However, we treated our samples further to remove possible unreacted starting material of Cr metal. Therefore, the enstatite pellets were manually crushed in an agate mortar, put in a 5N HCl solution at 80 °C for one hour and washed. The following treatment was further applied three times until the obtained solution did no longer show any green coloration, viz. put in a 5N HCl solution for 12 h at room temperature and for 1 h at 80 °C and washed. The powders were then dried for 24 h in a desiccator.

Chromium K-edge XANES spectra were recorded in fluorescence mode at room temperature at the European Synchrotron Radiation Facility (ESRF) on the undulator beamline ID26 (Gauthier et al. 1999; Solé et al. 1999). The storage ring

operating conditions were 6 GeV electron energy and 200–185 mA electron current. The excitation energy was selected using a fixed-exit Si(220) double-crystal monochromator. For all spectra, a reference foil (metallic Cr or Fe) was used to provide an internal energy calibration for the monochromator (first inflection point of the Cr K-edge and Fe K-edge set at 5989 and 7112 eV, respectively). We used two Si mirrors for the harmonics rejection of the incident X-ray beam (cut-off energy at 10 keV). XANES data were recorded in quick-scan mode by simultaneously scanning the monochromator angle and the undulator gap with a typical energy step of 0.25 eV and counting 20 ms per point. Each scan took 30 s and, in addition, a fast shutter was inserted, insuring that the sample was only exposed to the incident X-ray beam during acquisition. The spectra were acquired in fluorescence mode using a Si photo-diode and I<sub>0</sub> was monitored by measuring the fluorescence signal of a Kapton foil using a Si photo-diode. Periclase, ferropericlase, and Cr-MgSiO<sub>3</sub> perovskite samples were put onto carbon adhesive disks and positioned at 45° with respect to the beam. To check for homogeneity, spectra were acquired on different spots. In all periclase and ferropericlase samples except for sample 404, Cr metal was found in some positions, but these spectra were disregarded for this study. Reference XANES spectra were recorded on powder pellets of synthetic Cr-bearing enstatite (<sup>VI</sup>Cr<sup>2+</sup> in Mg<sub>0.90</sub>Cr<sub>0.10</sub>SiO<sub>3</sub>), chromite (<sup>VI</sup>Cr<sup>3+</sup> in FeCr<sub>2</sub>O<sub>4</sub>), and crocoite (<sup>IV</sup>Cr<sup>6+</sup> in PbCrO<sub>4</sub>). For the XANES spectra, a linear pre-edge background was subtracted followed by normalization to the edge jump. To extract the pre-edge features, the contribution of the edge jump to the pre-edge was modeled using a sum of Gaussian functions. Gaussian profiles were used to determine the energy position of the pre-edge components with the PeakFit4 software. To calculate the amount of Cr<sup>2+</sup> we used the method described by Berry and O'Neill (2004). The area of the derivative of the shoulder on the Cr<sup>2+</sup> absorption edge was determined using a Gaussian profile for the fit (Fig. 1c).

Mössbauer spectra were collected on ferropericlase samples that were in the form of compressed disk fragments. Spectra were recorded at room temperature (293 K) in transmission mode on a constant acceleration Mössbauer spectrometer with a nominal 370 MBq <sup>57</sup>Co high specific activity source in a 12 μm thick Rh matrix. The velocity scale was calibrated relative to 25 μm thick α-Fe foil using the positions certified for (former) National Bureau of Standards standard reference material no. 1541; line widths of 0.36 mm/s for the outer lines of α-Fe were obtained at room temperature. Spectra took 1–3 days each to collect, and were fitted using the commercially available fitting program NORMOS written by R.A. Brand (distributed by Wissenschaftliche Elektronik GmbH, Germany). Mössbauer spectra are similar to those already reported in the literature for periclase, and were fitted using Voigt lineshapes to two quadruple doublets corresponding to Fe<sup>2+</sup> and one quadruple doublet corresponding to Fe<sup>3+</sup> (Dobson et al. 1998). The metal phases in the samples were modeled with a magnetic sextet with hyperfine parameters close to those of pure iron (metal from the iron capsule) and a singlet (Fe-Ni alloy from the added metal). The hyperfine parameters of the singlet are consistent with those expected for a disordered Fe-Ni alloy quenched from high pressure (Guenzburger and Terra 2005), and the relative areas of the metal phases corrected for iron composition correlate well with estimates of metal abundance from the SEM observations. The value of Fe<sup>3+</sup>/ΣFe for ferropericlase was calculated from the relative area of the Fe<sup>3+</sup> absorption divided by the total area of ferropericlase absorption.

## RESULTS AND DISCUSSION

The use of XANES spectroscopy to determine the redox state and coordination number of transition metal cations generally relies on the analysis of the pre-edge features observed at the

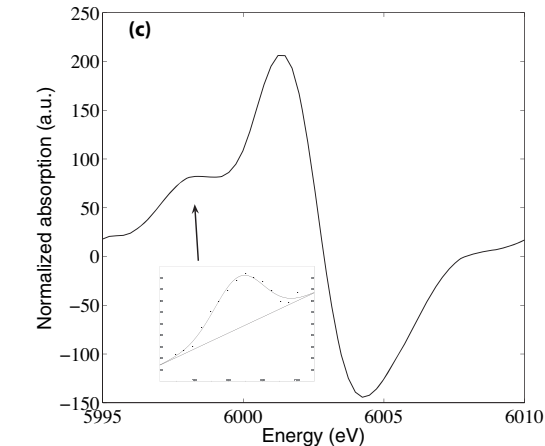
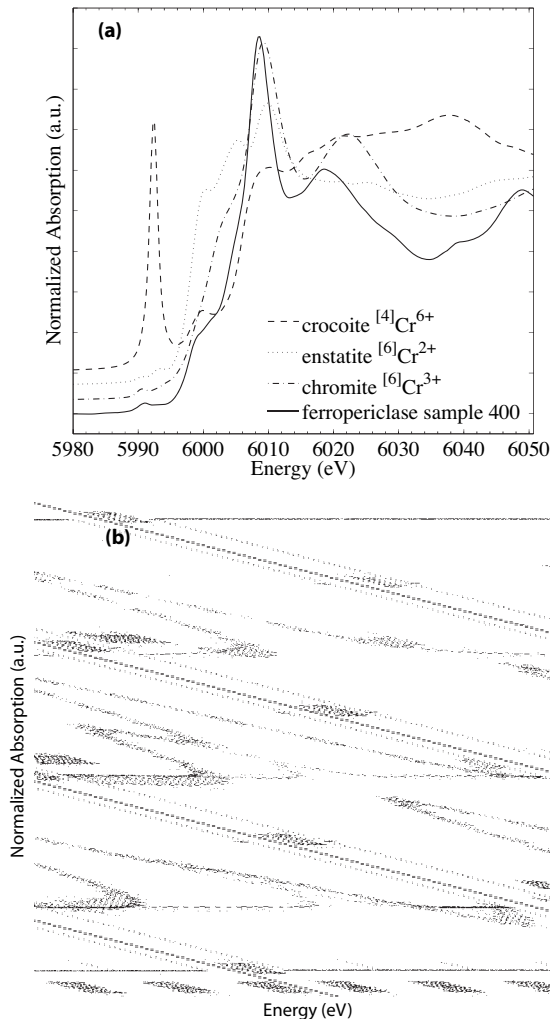


**FIGURE 1.** (a) Chromium  $K$ -edge XANES spectra of crocoite (dashed line), chromite (dash-dotted line), Cr-bearing enstatite (dotted line), and ferropericlase sample 400 (full line). (b) Fits of the background subtracted pre-edge peaks of chromite, Cr-bearing enstatite, and ferropericlase sample 400. (c) Fit of the area of the derivative of the shoulder on the  $\text{Cr}^{2+}$  absorption edge of ferropericlase sample 400 (see arrow).

**TABLE 2.** XANES features of Cr-bearing enstatite, chromite, crocoite, and ferropericlase sample 400

Sample	Pre-edge		Edge		
	Feature 1	Feature 2	Feature 1	Feature 2	Feature 3
enstatite	5990.5	5993.0	6000.1 (sh)	6005.2	6009.7
chromite	5990.6	*	6003.5 (sh)	6009.2	6022.3
crocoite	5992.4	5999.7	6009.7 (sh)	6016.4	6021.0
ferropericlase 400	5990.9	5992.6	6000.2 (sh)	6008.7	6018.7
perovskite	5990.5	5992.3	6001.3 (sh)	6009.1	6014.7

Note: Data are referred to the spectra reported in Figure 1.

\* A very weak shoulder around 5993.4 eV is observed (sh, shoulder).

low energy side of the edge (Fig. 1). These features are related to dipole and quadrupole transitions from the metal  $1s$  core state to metal  $3d$  with some contribution from  $4p$  depending on the local symmetry. Their intensity and energy therefore depend on the valence state and site symmetry of the metal cation (Calas and Petiau 1983; Farges et al. 2001; Giuli et al. 2003, 2004; Sutton et al. 2005; Westre et al. 1997; Wilke et al. 2001).

The experimental results of the XANES Cr  $K$ -edge of ferropericlase (sample 400) are compared with spectra of crocoite ( $^{\text{IV}}\text{Cr}^{6+}$ ), chromite ( $^{\text{VI}}\text{Cr}^{3+}$ ), and Cr-bearing enstatite ( $^{\text{VI}}\text{Cr}^{2+}$ ) (Figs. 1a and 1b, Table 2).

In the case of  $^{\text{IV}}\text{Cr}^{6+}$  a prominent pre-edge peak is observed at 5992.4 eV (Table 2) caused by a bound-state  $1s \rightarrow 3d$  transition, which is allowed for the non-centrosymmetric tetrahedral site (Peterson et al. 1997). The high intensity has been attributed to oxygen  $4p$  mixing into the metal  $3d$  orbitals providing some electric dipole allowed  $1s \rightarrow 4p$  character to the transition. Furthermore, this electric dipole coupled mechanism is much stronger than the electric quadrupole coupled mechanism, so that even a small amount of  $4p$  mixing into the  $3d$  orbitals can have

a significant effect on the intensity of the pre-edge peak (Westre et al. 1997). The strong pre-edge peak at 5992.4 eV is followed by a smaller one at 5999.7 eV. The XANES features of crocoite are labeled in Table 2.

In a centrosymmetric octahedral site the  $1s \rightarrow 3d$  transition is electric dipole forbidden by parity consideration. However, small pre-edge features are experimentally observed due to electric quadrupole coupling. In chromite (Fig. 1a and Table 2), this pre-edge peak occurs at 5990.6 eV and is followed by a very weak shoulder around 5993.4 eV. The absorption edge lies at 6009.2 eV and shows a shoulder at the low-energy side (Table 2). In Cr-bearing enstatite (Fig. 1a and Table 2), two distinct pre-edge features occur at 5990.5 and 5993.0 eV that are due to  $1s \rightarrow 3d$  electronic transitions. Burns (1993) related the separation by  $\sim 3$  eV of the pre-edge features to the 2–3 eV octahedral crystal field splitting between the  $t_{2g}$  and  $e_g$  levels. However, Glatzel et al. (2004) revealed using resonant inelastic X-ray scattering that this separation is due to strong electron-electron (multiplet) interactions. The prominent shoulder at 6000.1 eV, which precedes the absorption edge at 6005.2 eV, further characterizes the XANES spectrum of Cr-bearing enstatite. This feature is absent in chromite ( $^{\text{VI}}\text{Cr}^{3+}$ ) and appears as a shoulder in the studied Cr:MgO periclase samples (Figs. 1a and 2). Sutton et

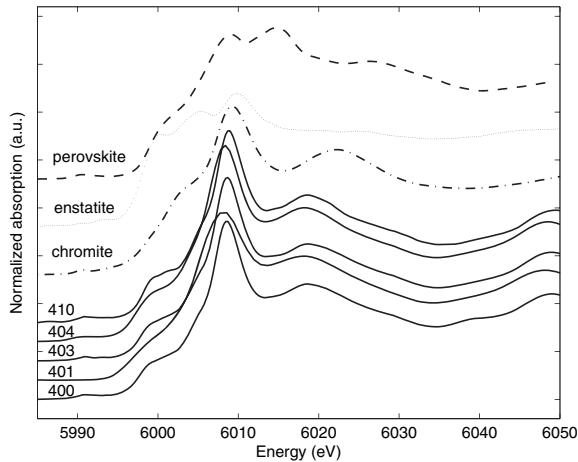


**FIGURE 2.** Chromium *K*-edge XANES spectra of chromite (dashed-dotted line), Cr-bearing enstatite (dotted line), Cr:MgSiO<sub>3</sub> perovskite (dashed line), and Cr:MgO periclase and Cr:(Mg,Fe)O ferropericlase samples (full lines).

al. (1993) attributed this shoulder in lunar olivine to the  $1s \rightarrow 4s$  electronic transition and used it to confirm the presence of Cr<sup>2+</sup>. The interpretation was picked up again by Berry et al. (2003) and Berry and O'Neill (2004). However, *s* orbitals are spherically symmetric and branching of  $a_{1g}$  into  $a_{1g}$  will only be allowed for very low symmetry. Furthermore, the high intensity of this peak as observed in Cr<sup>2+</sup>-bearing enstatite makes this interpretation rather implausible. In pyroxene, Cr<sup>2+</sup> occupies the octahedrally distorted M2 site (Papike et al. 2005). The degenerate  $e_g$  orbitals  $d_{z^2-y^2}$  and  $d_{z^2}$  are directed toward the octahedral oxygen ligands, so that uneven electron distributions in the high-spin  $d^4$  configuration (Cr<sup>2+</sup>) lead to strong electron-ligand interactions. Such  $\pi$ -bonding will result in strong peaks between the pre-edge and edge (de Groot F.M.F. and Glatzel P., personal communication). Since Jahn-Teller effect criteria predict Cr<sup>2+</sup> at more distorted octahedral sites, the presence of this feature around 6000.1 eV, together with the absence of a very strong pre-edge peak which is characteristic of tetrahedrally coordinated Cr, can be used to identify the presence of <sup>VI</sup>Cr<sup>2+</sup>.

The experimental Cr *K*-edge XANES spectra for the studied Cr:MgO and Cr:(Mg,Fe)O samples are depicted in Figure 2, where the spectra of Cr:MgSiO<sub>3</sub> perovskite, Cr<sup>2+</sup>-bearing enstatite and chromite are also shown. Visual inspection of this figure reveals subtle differences in the relative intensity of the lower-energy shoulder for the Cr:MgO samples. As outlined above, this absorption edge shoulder is diagnostic for Cr<sup>2+</sup>; hence we used the area of the corresponding peak in the derivative XANES spectra to quantify the amount of Cr<sup>2+</sup> (Berry and O'Neill 2004). The presence of this feature in periclase and Cr:MgSiO<sub>3</sub> perovskite would demonstrate the presence of Cr at the octahedral site. The results are shown in Figure 3 and labeled in Table 1. Note that an unambiguous interpretation of the edge features (Table 2) which are related to the medium-range order around the Cr cations would require *ab initio* electronic structure calculations (Gaudry et al. 2005) which are beyond the scope of the present study.

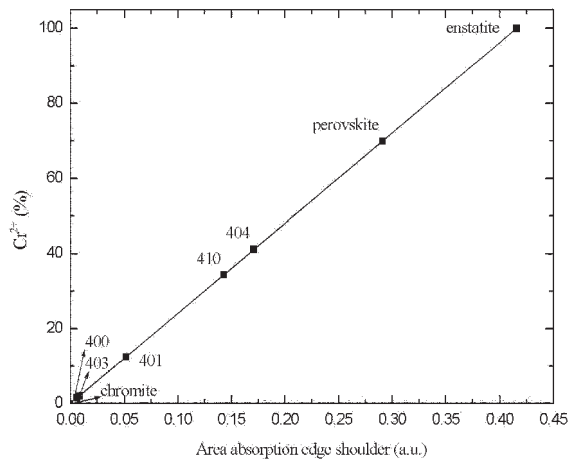


**FIGURE 3.** Increase in the area of the absorption edge shoulder (a.u.) as a function of Cr<sup>2+</sup> concentration (%) in the studied samples.

Mössbauer measurements (Fig. 4, Table 3) on ferropericlase synthesized in this study show that Fe<sup>3+</sup>/ΣFe is essentially at the detection limit (2%) for samples 400 and 401, and slightly higher for sample 403, where in the latter spectrum Fe<sup>3+</sup> absorption can be seen as a shoulder near 0.5 mm/s (Fig. 4). These results likely represent minimum values for Fe<sup>3+</sup>/ΣFe, since Berry et al. (2003) have shown that during quenching from high temperature Cr<sup>2+</sup> transforms to Cr<sup>3+</sup> in Fe-containing melt systems according to the reaction



and it is likely that a similar reaction will occur in ferropericlase during cooling from high temperature. Numerous studies have shown that Fe<sup>3+</sup> is incorporated into (Mg,Fe)O primarily through substitution on the octahedral site, where charge is balanced by the creation of cation vacancies (e.g., Valet et al. 1975; Hilbrandt and Martin 1998). Since both Fe<sup>2+</sup> and Fe<sup>3+</sup> occupy the same site in the crystal structure and Cr is expected to follow the same behavior due to size and crystal field considerations (e.g., Burns 1993), reaction 1 could easily occur as a function of temperature.

Our results show that Fe-free Cr:MgO samples contain significantly more Cr<sup>2+</sup> compared to Fe-containing samples, even under similar conditions of pressure, temperature and most probably oxygen fugacity (Table 2). Although starting materials for the Fe-free samples contained a higher fraction of trivalent cations (the Cr<sup>3+</sup>/Cr<sup>0</sup> ratio was 4:1) and metal in the run products was more difficult to detect than in the Fe-containing samples, we did find a small amount of metal in sample 410, and infer that the oxygen fugacity of the Fe-free Cr:MgO samples was probably not significantly oxidizing.

The most likely reason for this difference in relative Cr<sup>2+</sup> content between the Fe-free Cr:MgO samples and those containing Fe is the loss of Cr<sup>2+</sup> during cooling according to reaction 1. The additional Fe<sup>3+</sup> that was present at high temperature in ferropericlase is equal to the amount of Cr<sup>2+</sup> that was lost, and if the original relative Cr<sup>2+</sup> content [defined as Cr<sup>2+</sup>/(Cr<sup>2+</sup> + Cr<sup>3+</sup>)]

**TABLE 3.** Hyperfine parameters derived from room temperature Mössbauer spectra of Cr:(Mg,Fe)O ferropericlasite

Ferropericlasite sample no.	Fe <sup>2+</sup> *		Fe <sup>3+</sup>	Fe-rich metal			Cr-rich metal		Fe <sup>3+</sup> /ΣFe at%
	CS mm/s	QS mm/s	CS mm/s	CS mm/s	H T	A %	CS mm/s	A %	
400	1.05(5)	1.01(5)	0.40(3)	0.09(3)	33.5(5)	13(2)	-0.13	9(2)	2(2)
401	1.05(5)	0.99(5)	0.43(5)	0.11(5)	33.5(5)	11(3)	-0.15	4(2)	1(2)
403	1.04(5)	1.08(5)	0.37(2)	0.16(5)	32.6(4)	6(2)	-0.13	16(3)	5(2)

Notes: CS = center shift relative to  $\alpha$ -Fe; QS = quadruple splitting; H = hyperfine magnetic field; A = relative area.

\* Weighted mean square average of Fe<sup>2+</sup> values in ferropericlasite.

at high temperature in the ferropericlasite samples is assumed to have been the same as in the Fe-free samples (~40%; Table 1), we calculate high-temperature Fe<sup>3+</sup>/ΣFe ratios for samples 400, 401, and 403 of 3%, 2%, and 7%, respectively. These values are all within the range expected for  $f_{O_2}$  conditions near the iron-wüstite buffer based on experiments on Cr-free (Mg,Fe)O (McCammon 1993; McCammon et al. 1998), so a change in the relative Cr<sup>2+</sup> content during quenching for these samples seems likely.

In ferropericlasite when the synthesis temperature is increased from 1200 to 1400 °C at 12 GPa, the relative Cr<sup>2+</sup> content increases from 1.6 to 12.5% for the same bulk Cr concentration (Table 1). This behavior may be due to the temperature effect in stabilizing Cr<sup>2+</sup>, similar to observations in the system MgO-SiO<sub>2</sub>-Cr-O under terrestrial oxygen fugacity conditions where temperature plays an important role in the stability of Cr<sup>2+</sup> in olivine (Li et al. 1995). Another possibility, however, is that there was not sufficient Fe<sup>3+</sup> present in sample 401 at high temperature to oxidize all Cr<sup>2+</sup> to Cr<sup>3+</sup> during cooling, since the Fe<sup>3+</sup>/ΣFe ratio measured for that sample is essentially at the detection limit.

Compared to Cr:MgO, Cr:MgSiO<sub>3</sub> perovskite with 0.006 Cr pfu has a much higher relative Cr<sup>2+</sup> content, ~70%, even though this sample was synthesized under relatively oxidizing conditions (from MgSiO<sub>3</sub> and Cr<sub>2</sub>O<sub>3</sub> with trace amounts of water, in Pt capsule and LaCrO<sub>3</sub> furnace). This is surprising because one would have expected Cr<sup>3+</sup> to be stable in the octahedral site of the perovskite structure and/or to substitute for Si by coupling with H according to Si<sup>4+</sup> = Cr<sup>3+</sup> + H<sup>+</sup>. However, no OH was detected by micro-infrared spectroscopy in the perovskite crystals, which are >100 μm in diameter, even though the technique is capable to detect H contents at the level of 1 ppm wt H<sub>2</sub>O (see Bolfan-Casanova et al. 2000 for details about the infrared measurements). This result is consistent with previous experiments, which also indicate that Cr<sup>3+</sup> is not stable in perovskite (Andraut 2003). In these experiments, 25 mol% of XAlO<sub>3</sub> component was mixed with MgSiO<sub>3</sub> to study the coupled substitution of Al<sup>3+</sup> and other X<sup>3+</sup> cations (such as Y, Sc, Ga, Cr, and Fe) for Mg<sup>2+</sup> and Si<sup>4+</sup>. The only cation with which Al did not couple was Cr, suggesting that Cr was not trivalent in these experiments. The amount of Cr in the perovskite analyzed in this study is too low to allow determination of the site occupancy directly from electron microprobe analysis. However, the shape of the Cr edge for perovskite is very different from that of Cr in enstatite where Cr<sup>2+</sup> is hosted in octahedral coordination. This underlines the fact that Cr in perovskite is not substituting for silicon but for magnesium. It is even likely that under the more reducing conditions prevailing in the lower mantle, the valence state of Cr in magnesium silicate perovskite is mainly divalent. In this case, the substitution of Cr for Mg does not need to create any other defect in the structure. Compared to periclasite, it is possible that more Cr<sup>2+</sup>

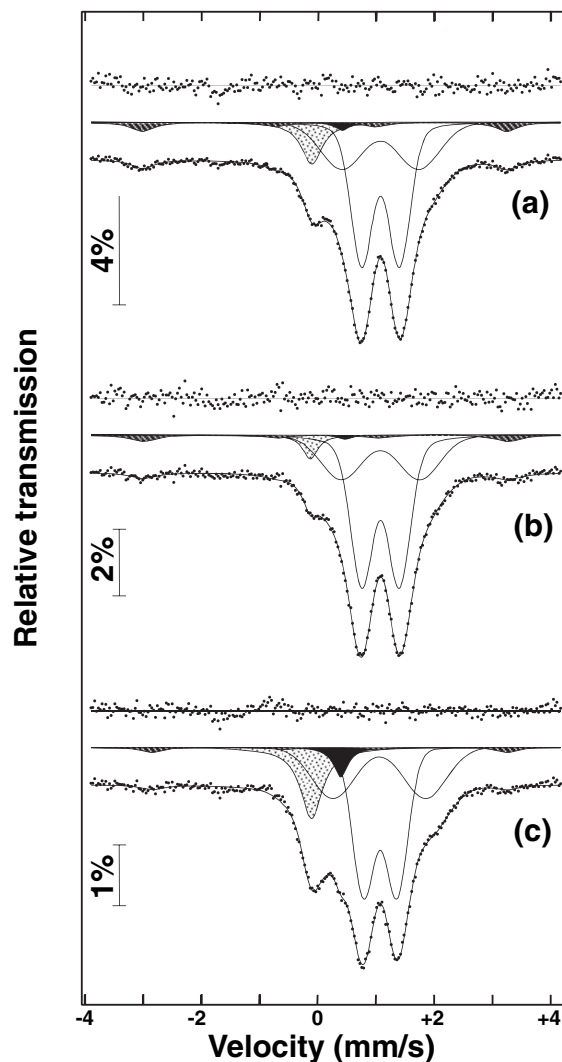


**FIGURE 4.** <sup>57</sup>Fe Mössbauer spectra at room temperature for Cr:(Mg,Fe)O ferropericlasite synthesized at low oxygen fugacity conditions: (a) sample 400, (b) sample 401, and (c) sample 403. Absorption due to Fe<sup>3+</sup>, Fe-rich metal, and Fe-Ni metal is shaded black, striped, and dotted, respectively, while unshaded peaks correspond to Fe<sup>2+</sup> in ferropericlasite.

(with respect to Cr<sup>3+</sup>) was incorporated into magnesium silicate perovskite as the result of the higher temperatures needed to synthesize perovskite.

The oxygen fugacity of the Earth's lower mantle is believed to be quite reducing, with the Fe<sup>3+</sup> concentration being controlled by the crystal chemistry of aluminous (Mg,Fe)(Si,Al)O<sub>3-x</sub> perovskite

(McCammon 2005). The excess  $\text{Fe}^{3+}$  required by the perovskite phase is likely balanced by the disproportionation of iron according to  $3 \text{Fe}^{2+} = 2 \text{Fe}^{3+} + \text{Fe}^0$  (Frost et al. 2004). Under these circumstances, it is likely that a portion of Cr will be divalent. This is important because chromium has been always considered to be present in the Earth's interior as  $\text{Cr}^{3+}$ . As a consequence, the partitioning of Cr between mineral phases will likely be affected by the oxidation state of Cr, since  $\text{Cr}^{2+}$  has a much larger ionic radius than  $\text{Cr}^{3+}$  (0.80 Å compared to 0.615 Å for octahedral coordination) (Shannon and Prewitt 1970).

Diamonds, thought to originate in the lower mantle, frequently contain ferropericlasite inclusions that can be used to qualitatively evaluate oxygen fugacity conditions during diamond formation (McCammon et al. 2004). Using Mössbauer spectroscopy to determine  $\text{Fe}^{3+}/\Sigma\text{Fe}$ , the concentration of cation vacancies can be determined using the charge balance condition

$$\square = \frac{1}{2} (\text{Fe}^{3+} + \text{Al} + \text{Cr}^{3+} + \text{Na}) \quad (2)$$

where  $\square$  is the number of vacancies on the octahedral cation site, which increases with increasing oxygen fugacity as a function of total iron concentration (McCammon et al. 2004 and references therein). The calculation of cation vacancies according to Equation 2 is not changed if electron exchange occurs according to reaction 1 during cooling of the diamonds, because the loss of  $\text{Fe}^{3+}$  during cooling is balanced by the addition of an equal amount of  $\text{Cr}^{3+}$ .

An independent measure of oxygen fugacity conditions during diamond formation could be obtained by a determination of the relative  $\text{Cr}^{2+}$  content of ferropericlasite inclusions. For example, the chromium content of lower mantle ferropericlasite in diamonds from Kankan, Guinea ranges from 0.3 to 0.8 wt% measured as  $\text{Cr}_2\text{O}_3$  (Stachel et al. 2000), which combined with Mössbauer determinations of  $\text{Fe}^{3+}/\Sigma\text{Fe}$  show that the cation abundance of Cr is comparable to the abundance of  $\text{Fe}^{3+}$ . This means that in the case of low oxygen fugacity, since  $\text{Cr}^{2+}$  and  $\text{Fe}^{2+}$  would be favored at high temperature,  $\text{Cr}^{2+}$  could be partly preserved during cooling if there were not sufficient  $\text{Fe}^{3+}$  available for reaction 1 to occur. On the other hand if oxygen fugacity were high, the stability of both  $\text{Cr}^{3+}$  and  $\text{Fe}^{3+}$  at high temperature would mean that no  $\text{Cr}^{2+}$  would be expected after cooling. The opportunity to distinguish between reducing and oxidizing conditions during diamond formation using the relative  $\text{Cr}^{2+}$  content of ferropericlasite inclusions would be best for lower mantle ferropericlasite inclusions with Cr contents at the higher end of the range of observed values (e.g., >0.5 wt%  $\text{Cr}_2\text{O}_3$ ) and iron contents at the lower end of the observed range (e.g., <20 wt% FeO).

#### ACKNOWLEDGMENTS

We wish to thank the staff of beamline ID26 (ESRF, Grenoble, France) for assistance during the XANES measurements and Leverhulme Trust for financial support with the enstatite synthesis. We appreciate the helpful reviews by Simona Quartieri and by an anonymous colleague.

#### REFERENCES CITED

Allègre, C.J., Poirier J.-P., Humler E., and Hofmann A.W. (1995) The chemical composition of the Earth. *Earth and Planetary Science Letters*, 134, 515–526  
 Andraut, D. (2003) Cationic substitution in  $\text{MgSiO}_3$  perovskite. *Physics of the Earth and Planetary Interiors*, 136, 67–78.

Berry, A.J. and O'Neill, H.St.C. (2004) A XANES determination of the oxidation state of chromium in silicate glasses. *American Mineralogist*, 89, 790–798.  
 Berry, A.J., Shelley, J.M.G., Foran, G.J., O'Neill, H.S., and Scott, D.R. (2003) A furnace design for XANES spectroscopy of silicate melts under controlled oxygen fugacities and temperatures to 1773 K. *Journal of Synchrotron Radiation*, 10, 332–336.  
 Bolfan-Casanova, N., Keppler, H., and Rubie, D.C. (2000) Partitioning of water between mantle phases in the system  $\text{MgO-SiO}_2\text{-H}_2\text{O}$  up to 24 GPa: Implications for the distribution of water in the Earth's mantle. *Earth and Planetary Science Letters*, 182, 209–221.  
 ——— (2003) Water partitioning at 660 km depth and evidence for very low water solubility in magnesium silicate perovskite. *Geophysical Research Letters*, 30(17), 1905, DOI:10.1029/2003GL017182.  
 Burns, R.G. (1993) *Mineralogical applications of the crystal field theory*, 2<sup>nd</sup> edition. Cambridge University Press, U.K.  
 Calas, G. and Petiau, J. (1983) Coordination of iron in oxide glasses through High-Resolution K-Edge spectra—Information from the pre-edge. *Solid State Communications*, 48, 625–629.  
 Dobson, D.P. and Brodholt, J.P. (2000) The electrical conductivity of the lower mantle phase magnesio-wustite at high temperatures and pressures. *Journal of Geophysical Research-Solid Earth*, 105(B1), 531–538.  
 Dobson, D.P., Cohen, N.S., Pankhurst, Q.A., and Brodholt, J.P. (1998) A convenient method for measuring ferric iron in magnesio-wustite ( $\text{MgO-Fe}_{1-x}\text{O}$ ). *American Mineralogist*, 83, 794–798.  
 Farges, F., Brown, G.E., Petit, P.E., and Munoz, M. (2001) Transition elements in water-bearing silicate glasses/melts. Part I. A high-resolution and anharmonic analysis of Ni coordination environments in crystals, glasses, and melts. *Geochimica et Cosmochimica Acta*, 65, 1665–1678.  
 Frost, D.J., Liebske, C., Langenhorst, F., McCammon, C.A., Tronnes, R.G., and Rubie, D.C. (2004) Experimental evidence for the existence of iron-rich metal in the Earth's lower mantle. *Nature*, 428, 409–412.  
 Gaudry, E., Cabaret, D., Sainctavit, P., Brouder, C., Mauri, F., Goulon, J., and Rogalev, A. (2005) Structural relaxations around Ti, Cr and Fe impurities in  $\alpha\text{-Al}_2\text{O}_3$  probed by x-ray absorption near-edge structure combined with first-principles calculations. *Journal of Physics—Condensed Matter*, 17, 5467–5480.  
 Gauthier, C., Solé, V.A., Signorato, R., Goulon, J., and Moguiline, E. (1999) The ESRF beamline ID26: X-ray absorption on ultra dilute sample. *Journal of Synchrotron Radiation*, 6, 164–166.  
 Giuli, G., Paris, E., Pratesi, G., Koeberl, C., and Cipriani, C. (2003) Iron oxidation state in the Fe-rich layer and silica matrix of Libyan Desert Glass: A high-resolution XANES study. *Meteoritics and Planetary Science*, 38, 1181–1186.  
 Giuli, G., Paris, E., Mungall, J., Romano, C., and Dingwell, D. (2004) V oxidation state and coordination number in silicate glasses by XAS. *American Mineralogist*, 89, 1640–1646.  
 Glatzel, P., Bergmann, U., Yano, J., Visser, H., Robblee, J.H., Gu, W.W., de Groot, F.M.F., Christou, G., Pecoraro, V.L., Cramer, S.P., and Yachandra, V.K. (2004) The electronic structure of Mn in oxides, coordination complexes, and the oxygen-evolving complex of photosystem II studied by resonant inelastic X-ray scattering. *Journal of the American Chemical Society*, 126, 9946–9959.  
 Goncharov, A.F., Struzhkin, V.V., and Jacobsen, S.D. (2006) Reduced radiative conductivity of low-spin (Mg,Fe)O in the lower mantle. *Science*, 312, 1205–1208.  
 Guenzburger, D. and Terra, J. (2005) Theoretical study of magnetism and Mössbauer hyperfine interactions in ordered FeNi and disordered fcc Fe-rich Fe-Ni alloys. *Physical Review B*, 72(2), 024408.  
 Hilbrandt, N. and Martin, M. (1998) High temperature point defect equilibria in iron-doped MgO: An in situ Fe-K XAFS study on the valence and site distribution of iron in  $(\text{Mg}_{1-x}\text{Fe}_x)\text{O}$ . *Berichte der Bunsen-Gesellschaft für Physikalische Chemie*, 102, 1747–1759.  
 Li, J. and Agee, C.B. (1996) Geochemistry of mantle-core differentiation at high pressure. *Nature*, 381, 686–689.  
 Li, J.P., O'Neill, H.S., and Seifert, F. (1995) Subsolidus phase-relations in the system  $\text{MgO-SiO}_2\text{-Cr-O}$  in equilibrium with metallic Cr, and their significance for the petrochemistry of chromium. *Journal of Petrology*, 36, 107–132.  
 Mackwell, S., Bystricky, M., and Sproni, C. (2005) Fe-Mg interdiffusion in (Mg,Fe)O. *Physics and Chemistry of Minerals*, 32, 418–425.  
 McCammon, C.A. (1993) Effect of pressure on the composition of the Lower Mantle end member  $\text{FexO}$ . *Science*, 259, 5091.  
 ——— (2005) The paradox of mantle redox. *Science*, 309, 1816–1816.  
 McCammon, C.A., Peyronneau, J., and Poirier, J.P. (1998) Low ferric iron content of (Mg,Fe)O at high pressures and temperatures. *Geophysical Research Letters*, 25, 1589–1592.  
 McCammon, C.A., Stachel, T., and Harris, J.W. (2004) Iron oxidation state in lower mantle mineral assemblages—II. Inclusions in diamonds from Kankan, Guinea. *Earth and Planetary Science Letters*, 222, 423–434.  
 O'Neill, H.St.C. and Palme, H. (1998) Composition of the silicate earth: implications for accretion and core formation. In I. Jackson, Ed., *The Earth's Mantle-Composition, Structure and Evolution*, p. 3–126. Cambridge University Press, U.K.

- Papike, J.J., Karner, J.M., and Shearer, C.K. (2005) Comparative planetary mineralogy: Valence state partitioning of Cr, Fe, Ti, and V among crystallographic sites in olivine, pyroxene, and spinel from planetary basalts. *American Mineralogist*, 90, 277–290.
- Peterson, M.L., Brown, G.E., Parks, G.A., and Stein, C.L. (1997) Differential redox and sorption of Cr(III/VI) on natural silicate and oxide minerals: EXAFS and XANES results. *Geochimica et Cosmochimica Acta*, 61, 3399–3412.
- Shannon, R.D. and Prewitt, C.T. (1970) Revised values of effective ionic radii. *Acta Crystallographica Section B—Structural Crystallography and Crystal Chemistry*, B 26, 1046.
- Solé, V.A., Gauthier, C., Goulon, J., and Natali, F. (1999) Undulator QEXAFS at the ESRF beamline ID26. *Journal of Synchrotron Radiation*, 6, 174–175.
- Stachel, T., Harris, J.W., Brey, G.P., and Joswig, W. (2000) Kankan diamonds (Guinea) II: lower mantle inclusion parageneses. *Contributions to Mineralogy and Petrology*, 140, 16–27.
- Sutton, S.R., Jones, K.W., Gordon, B., Rivers, M.L., Bajt, S., and Smith, J.V. (1993) Reduced chromium in olivine grains from lunar basalt 15555—X-Ray Absorption Near Edge Structure (XANES). *Geochimica et Cosmochimica Acta*, 57, 461–468.
- Sutton, S.R., Karner, J., Papike, J., Delaney, J.S., Shearer, C., Newville, M., Eng, P., Rivers, M., and Dyar, M.D. (2005) Vanadium *K* edge XANES of synthetic and natural basaltic glasses and application to microscale oxygen barometry. *Geochimica et Cosmochimica Acta*, 69, 2333–2348.
- Valet, P.M., Pluschkell, W., and Engell, H.J. (1975) Equilibria between MgO-FeO-Fe<sub>2</sub>O<sub>3</sub> solid-solutions and oxygen. *Archiv für das Eisenhüttenwesen*, 46, 383–388.
- Westre, T.E., Kennepohl, P., DeWitt, J.G., Hedman, B., Hodgson, K.O., and Solomon, E.I. (1997) A multiplet analysis of Fe *K*-edge 1s → 3d pre-edge features of iron complexes. *Journal of the American Chemical Society*, 119, 6297–6314.
- Wilke, M., Farges, F., Petit, P.E., Brown, G.E., and Martin, F. (2001) Oxidation state and coordination of Fe in minerals: An Fe *K*-XANES spectroscopic study. *American Mineralogist*, 86, 714–730.